

Article

Genotoxic Changes to Rodent Cells Exposed *in Vitro* to Tungsten, Nickel, Cobalt and Iron

Stephanie Bardack ¹, Clifton L. Dalgard ², John F. Kalinich ³ and Christine E. Kasper ^{4,5,*}

¹ Office of the Assistant Secretary for Preparedness and Response, Department of Health and Human Services, Washington, D.C. 20201, USA; E-Mail: Stephanie.Bardack@hhs.gov

² Department of Anatomy, Physiology, and Genetics, School of Medicine, Uniformed Services University of the Health Sciences, 4301 Jones Bridge Road, Bethesda, MD 20814, USA; E-Mail: clifton.dalgard@usuhs.edu

³ Armed Forces Radiobiology Research Institute, Uniformed Services University of the Health Sciences, 8901 Wisconsin Avenue, Bethesda, MD 20889, USA; E-Mail: john.kalinich@usuhs.edu

⁴ Daniel K. Inouye Graduate School of Nursing, Uniformed Services University of the Health Sciences, 4301 Jones Bridge Road, Bethesda, MD 20814, USA

⁵ Department of Veterans Affairs, Office of Nursing Services, 810 Vermont Avenue, N.W., Washington, DC 20420, USA

* Author to whom correspondence should be addressed; E-Mail: christine.kasper@va.gov; Tel.: +1-202-422-2679; Fax: +1-301-295-1707.

Received: 27 December 2013; in revised form: 21 February 2014 / Accepted: 25 February 2014 / Published: 10 March 2014

Abstract: Tungsten-based materials have been proposed as replacements for depleted uranium in armor-penetrating munitions and for lead in small-arms ammunition. A recent report demonstrated that a military-grade composition of tungsten, nickel, and cobalt induced a highly-aggressive, metastatic rhabdomyosarcoma when implanted into the leg muscle of laboratory rats to simulate a shrapnel wound. The early genetic changes occurring in response to embedded metal fragments are not known. In this study, we utilized two cultured rodent myoblast cell lines, exposed to soluble tungsten alloys and the individual metals comprising the alloys, to study the genotoxic effects. By profiling cell transcriptomes using microarray, we found slight, yet distinct and unique, gene expression changes in rat myoblast cells after 24 h metal exposure, and several genes were identified that correlate with impending adverse consequences of ongoing exposure to weapons-grade tungsten

alloy. These changes were not as apparent in the mouse myoblast cell line. This indicates a potential species difference in the cellular response to tungsten alloy, a hypothesis supported by current findings with *in vivo* model systems. Studies examining genotoxic-associated gene expression changes in cells from longer exposure times are warranted.

Keywords: genotoxic; tungsten; military; fragments; shrapnel; cancer

1. Introduction

Retained or embedded fragment wounds (shrapnel) have long been a hazard of war. Modern warfare and its associated technological advances have produced munitions that have increased in both range and lethality. So too have the devices designed to protect the warfighter from the effects of these same munitions. Where previously an injury from exploded ordnances would likely have proved fatal, advances in both protective equipment and medical treatment have rendered even the most severe injuries survivable.

One practice, that of removing retained or embedded fragments, has changed little over time. Military medical practice has long held that fragments posing no immediate threat to the individual can remain in place. However, the composition of munitions has changed, and many modern munitions may pose a health hazard via long-term exposure to the retained embedded fragments.

What has also changed is the science and study of genomics and molecular biology, including research on cellular changes down to the level of genetic composition and alteration. The body of knowledge and evidence related to genetic changes and disease processes is expanding at an exponential rate. Where previous science could only postulate on correlative associations, emerging research in genomics is now providing causative evidence of oncogenic changes initiated by exposure to various substances. Additionally, as military and civilian personnel increasingly face survivable injuries and embedded fragments composed of potentially harmful materials, it is critical that healthcare providers be aware of current policy and practice.

Many metals occur naturally in the environment and are found in the human body at sub-toxic levels. However, an increase in metal exposure may cause cellular changes, activate oncogenes or inactivate tumor suppressor genes. Common industrial exposure to heavy metals can occur by ingestion, inhalation and dermal absorption. However, in a combat setting, exposure can also occur via tissue penetration by metal fragments. Although many metals are found in combat situations that could potentially result in embedded fragment wounds, two recently used materials are of major concern to the U.S. Department of Defense.

Depleted uranium (DU) was once the metal of choice for U.S. military kinetic-energy munitions. DU saw its first widespread combat use in the First Persian Gulf War. A number of “friendly-fire” incidents left several U.S. personnel with wounds containing embedded DU fragments. As a result of the unique chemical and radiological properties of DU, concern was raised over the long-term health effects of these embedded fragments. A 1993 study conducted by the Armed Forces Radiobiology Research Institute at the request of the U.S. Army Surgeon General reviewed the potential hazards of embedded DU and concluded there were “sufficient uncertainties about the long-term chemical and

radiological effects of embedded DU to warrant the initiation of animal toxicology pilot studies” [1]. Since that time, a large body of research has evaluated the potential long-term health effects of embedded DU fragments [2–20].

Nonetheless, concern still exists over the long-term health and environmental effects of depleted uranium. As a result, a search for a suitable replacement for DU in armor-penetrating munitions was undertaken and several tungsten-based materials were identified. However, this was not the first combat use of tungsten. As early as the 1950s, the U.S. military had used tungsten carbide in armor-piercing munitions. As armor improved, tungsten carbide was replaced with an alloy of 97.5% tungsten and 2.5% binder material with a density of 18.5 g/mL [21]. Today, the composition of weapons-grade tungsten alloy varies, but some of the most widely used formulations are 91%–93% tungsten, 3%–5% nickel, and either 2%–4% cobalt or iron [22].

For years, tungsten was considered “relatively safe” from a toxicological perspective [23]. However, using a rodent model system designed to investigate the health effects of embedded metal fragments, Kalinich *et al.* demonstrated that a military-grade tungsten alloy comprised of tungsten, nickel, and cobalt induced aggressive metastatic rhabdomyosarcomas in the leg muscles of F344 laboratory rats [24]. A study characterizing the aerosols produced in a vehicle struck by a tungsten penetrator also raised concerns over the health effects associated with exposure to the aerosolized metal particles [25]. The authors concluded that further research was needed to determine the extent of risk.

Embedded fragments are generally not surgically removed unless they pose a future health risk. However, the findings of Kalinich *et al.* [24] raises new concerns about long-term health effects of retained tungsten alloy fragments. As a result, the U.S. Department of Defense (DOD) mandated that all fragments removed from DOD personnel be analyzed for metal content [26]. However, questions still remain on which embedded fragments pose a health risk and which can remain in place without concern. This study seeks to address some of those concerns with respect to embedded tungsten alloy fragments. The research described herein is designed to explore and assess the genotoxic effects of weapons-grade tungsten alloy on living cells. The purpose is to identify early genetic changes induced by exposure to weapons-grade tungsten alloy that may be used as an indicator of future carcinogenicity. Such information could provide healthcare providers with the knowledge required to make informed treatment decisions when dealing with embedded fragment injuries. In addition, this information will guide any changes in policy or clinical practice on the removal of embedded fragments in general and weapons-grade tungsten alloy fragments in particular. In this *in vitro* study, we utilized cultured rodent muscle cell lines to assess the potential genotoxic-associated gene expression changes of the metals comprising two military-relevant tungsten alloys.

2. Experimental Section

2.1. Cell Culture

The rat myoblast cell line L6 (CRL #1458) and mouse myoblast cell line C2C12 (CRL #1772) were both purchased from the American Type Culture Collection (Manassas, VA, USA). Cells were grown as a monolayer in Dulbecco’s Modified Eagle’s Medium (DMEM, Invitrogen, Grand Island, NY, USA) supplemented with 10% fetal bovine serum (Invitrogen) and 1% penicillin-streptomycin (Invitrogen) at

37 °C in a humidified atmosphere of 5% CO₂ in air. Cultures were routinely fed every 3–4 days, and passaged weekly. Experiments were conducted using cells at 80%–90% confluency as determined by microscopic observation.

2.2. Test Metals and Exposure Groups

Soluble test metals included the following compounds: CoCl₂·6H₂O, NiCl₂·6H₂O, FeCl₃·6H₂O, Na₂WO₄·2H₂O, and TaCl₅. All compounds were purchased from Sigma-Aldrich (St. Louis, MO, USA). Because the WNiCo and WNiFe compounds are not commercially available, they were reconstituted in the laboratory at 91% W, 6% Ni, and 3% Co or Fe using the method of Miller *et al.* [22]. All metal solutions were prepared in sterile DMEM immediately prior to use. After thorough mixing, the metal solutions were added to the cells to a final metal concentration of 10 µg/mL. There were eight treatment groups: control (no metal), Ta, W, Ni, Co, Fe, WNiCo, and WNiFe. Cells were treated for 24 h under the conditions described above. Metal treatments, under these experimental conditions, did not adversely affect the cells as determined by microscopic observation and previously published studies [27].

2.3. RNA Isolation

After metal exposure for the indicated duration, the medium was removed and the cells were washed twice with Dulbecco's Phosphate Buffered Saline (Invitrogen). Total RNA was isolated from the cells using commercially available kits (RNeasy Mini Kit; Qiagen, Valencia, CA, USA) and following the manufacturer's protocol. Total RNA concentration and purity were determined by measuring the absorbance at 260 and 280 nm using a NanoDrop ND-1000 spectrophotometer (NanoDrop Technologies, Inc., Wilmington, DE, USA). RNA samples with a 260/280 and 260/230 ratio of greater than 1.9 were used for microarray analysis. Samples were stored at –80 °C until needed.

2.4. Microarray Analysis

RNA samples were sent to the Genomics Core of the Lerner Research Institute at the Cleveland Clinic (Cleveland, OH, USA) for whole genome RNA expression analysis. The integrity of the RNA was assessed using the Agilent 2100 Bioanalyzer (Santa Clara, CA, USA), and samples with RNA Integrity Number (RIN) greater than 9.0 were then processed and labeled before hybridizing to the RatRef-12 v1.0 Expression BeadChip (Illumina, San Diego, CA, USA) for the rat RNA and the MouseRef-8 v2.0 Expression BeadChip for the mouse RNA (Illumina). BeadChips were imaged using a BeadArray Reader (Illumina), and raw data output was generated using the GenomeStudio software package (Illumina). Relevant output files were accessed via FTP from the Genomics Core file servers. The dataset for this study was generated using raw data from the probe-level, quantile-normalized BeadArray data file. The dataset was analyzed at the level of the individual probes, since multiple probes interrogate transcripts from individual genes. This data file was used, as opposed to gene level or non-quantile normalized data files, because normalized data accounts for possible variations of sample input on the BeadArray and also allows for the detection of various isoforms of genes. The complete probe datasets were then evaluated using hierarchical clustering and comparative marker

selection (CMS) analyses with GenePattern software [28] (Broad Institute, Cambridge, MA, USA) to determine if there were any significant differences in expression between the experimental groups.

2.5. Quantitative Real-Time PCR

To confirm the expression validity of the selected genes found in the microarray data, RT-PCR and quantitative PCR were run on the selected genes and a housekeeping gene (HPRT). Primer design was based on the transcript RefSeq number, and performed using Primer-BLAST (NCBI, Bethesda, MD, USA). Primers were designed to span an exon-exon boundary to prevent amplification of possible genomic DNA contamination. The primers were obtained from Integrated DNA Technologies (Coralville, IA, USA), and maintained at 4 °C. RT-PCR reactions were performed to verify the production of a single amplicon of specific size. The primers used are listed in Table 1.

Table 1. Primer sequences used in qPCR.

Gene Symbol	Accession #	Forward Primer Sequence	Reverse Primer Sequence
AP2A1	NM_001107511.1	GCTGTGTCTCGCCTAAGCCGG	AGAGCCAGGGTGCAGGAACGA
CHRND	NM_019298.1	AACCGCAGTTACCCATTGAGTGG	CATTGGGACACTGGGGTCCACG
ERG1	NM_012551.2	AGCGAACAACCCTACGAGCACCT	TCTCCACCAGCGCCTTCTCGTTA
FBXW5	NM_001025730.1	GCGAGCACACCGTGCCTACA	CCGATCTTCAGCCCCACTGGC
FN3K	NM_001109051.1	CCGAGAGACACAAGAAGTGTGGTCA	ATGGAGCAGGGCAGGGACAATC
FOS	NM_022197.2	CCCACGGTGACAGCCATCTCC	GCACCAGCCACTGCAGGTCTG
GALNT2	NM_001106196.1	ATCAGGTTGCAGGGCTGCCG	GTTGCTCCCCACGTGTCCGA
HPRT1	NM_012583.2	CGAAGTGTGGATACAGGCCAGACT	TTGGCTTTTCCACTTTCGCTGATG
NMT2	NM_207590.1	TGGTTCCTCCCCAGGGAGCAC	CGGGGTGGTGCATAACCGTGG
POLR3E	NM_001108503.1	GAGAGAGGGAGGCGCCAATG	GAGCCTGCTCTGACTCTGGCCT

cDNA was generated via reverse transcription (RT) with 1 µg of total RNA and an iScript Reverse Transcription kit (BioRad, Hercules, CA, USA) using the GeneAmp PCR System 9700 (Applied Biosystems, Carlsbad, CA, USA). The protocol for running the RT is as follows:

- Step 1: 5:00 at 25 °C;
- Step 2: 30:00 at 42 °C;
- Step 3: 5:00 at 85 °C;
- Step 4: Hold at 4 °C.

The selected gene expression values from the microarray analysis were validated by real-time qPCR using SsoFast EvaGreen Supermix (Bio-Rad) and the C1000 Thermal Cycler (BioRad) with the following protocol:

- Step 1: Run at 98 °C for 2:00;
- Step 2: Run at 98 °C for 0:05;
- Step 3: Run at 55 °C for 0:02;
- Step 4: Repeat (×40) steps 2 and 3
- Step 5: Determine melt curve from 65–95 °C in 0.5 °C increments for 0:05 each.

The amount of transcript measured in each sample was normalized to the housekeeping gene HPRT1. Comparative values of the control group were used to calculate fold change, and results are expressed as the fold change of normalized level of mRNA in the treatment over the value obtained in normal controls.

3. Results

Previous research showed that embedded pellets of a military-grade alloy of tungsten/nickel/cobalt induced highly-aggressive metastatic rhabdomyosarcomas in laboratory rats [25], while one composed of tungsten/nickel/iron did not [29]. To determine the genotoxic-associated transcriptome alteration potential of these materials, we tested soluble forms of the alloys, as well as the individual metals, using cultured rat and mouse myoblast cell lines and commercially available gene chips. The results obtained were compared to untreated controls and tantalum-treated cells. Tantalum has been shown to be an inert non-reactive metal that has been used in medical implants [30,31].

3.1. Metal Treatment of Myoblast Cell Lines

Prior to initiation of this study, the effect of metal concentration and exposure time on the L6 and C2C12 cells was determined. As previously shown by others [27], metal concentrations of less than 100 μg of metal/mL of growth medium with exposure times of 72 h or less did not affect the growth or viability of the L6 and C2C12 myoblast lines. To avoid confounding effects of cytotoxicity, a metal concentration of 10 μg /mL and a 24 h exposure time were selected for use in this study.

3.2. Probe Characterizations

The Illumina RatRef-12 array contains 22,523 probes on the bead chip, representing 21,910 unique genes. BeadArray technology allows for a statistical determination of accurate detection for each transcript by calculating signal intensity variance for replicate beads [32]. We hypothesized that the low concentration and short duration exposures would not result in a robust change in molecular phenotype and significant increase in the number of genes expressed in the differentially treated cells. Therefore, we determined the absolute number of expressed genes in each exposure condition. In this study, 8,193 probes were determined to be accurately detected in all eight exposure groups at $p \leq 0.05$ (36% of all probes). A detection p -value of ≤ 0.05 signifies a 5% possibility that the resulting signal value for a given feature (probe) is inaccurate. The 8,193 probes corresponded to 8038 unique genes accurately detected at $p \leq 0.05$. By comparison, raising the p -value cut off to ≤ 0.01 (a 1% possibility of inaccurate detection) resulted in 7,204 probes (representing 6,960 unique genes) being accurately detected in all eight exposure groups. In order to determine whether or not metal exposure dramatically changed the transcriptome (RNA) of the cells, the total number of differentially expressed rat genes was analyzed, and no significant differences were observed in a comparison of the number of differentially expressed genes in each of the eight sample groups between the p -value cutoff of ≤ 0.05 or ≤ 0.01 (Figure 1 and Table 2). This suggests only a small effect in all treatment groups from metal exposure after 24 h and early gene expression changes are occurring while molecular and cellular phenotypes are not robustly altered.

Figure 1. Rat data comparison between actual numbers of features accurately expressed in each exposure group at the detection p -value ≤ 0.05 and ≤ 0.01 .

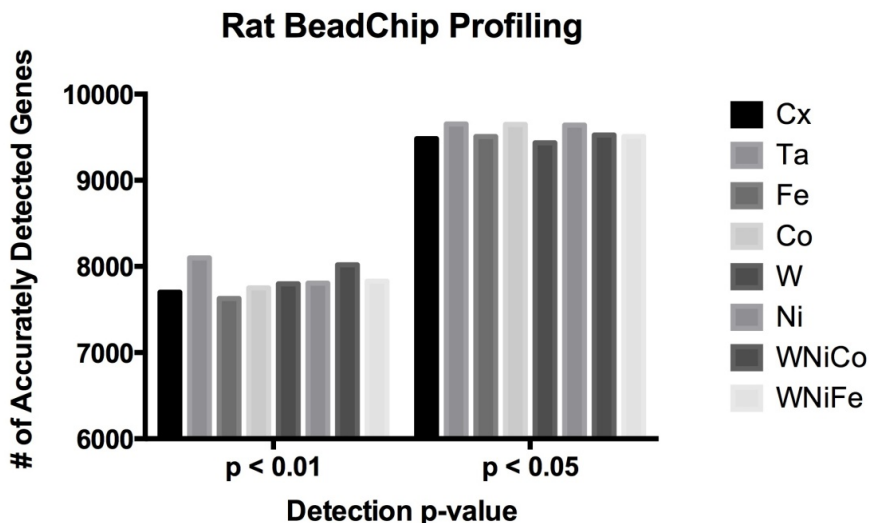


Table 2. Rat data comparison between actual numbers of features accurately expressed in each exposure group at the detection p -value ≤ 0.05 and ≤ 0.01 .

	Cx	Ta	Fe	Co	W	Ni	WNiCo	WNiFe
$p \leq 0.05$	9482	9652	9507	9647	9436	9640	9526	9507
$p \leq 0.01$	7701	8098	7629	7750	7799	7806	8020	7829

The Illumina MouseRef-8 (v2.0) array contains 25,697 probes representing over 19,100 unique genes. On these 10,048 probes (39% of all probes) were accurately detected in all eight exposure groups at a detection p value of ≤ 0.05 , which corresponded to 7578 unique genes. At $p \leq 0.01$, 9048 probes were accurately detected, corresponding to 6902 unique genes. No significant differences were observed in a comparison of the number of differentially expressed genes between the eight sample groups (Figure 2 and Table 3).

Figure 2. Mouse data comparison between actual numbers of features accurately expressed in each exposure group at the detection p -value ≤ 0.05 and ≤ 0.01 .

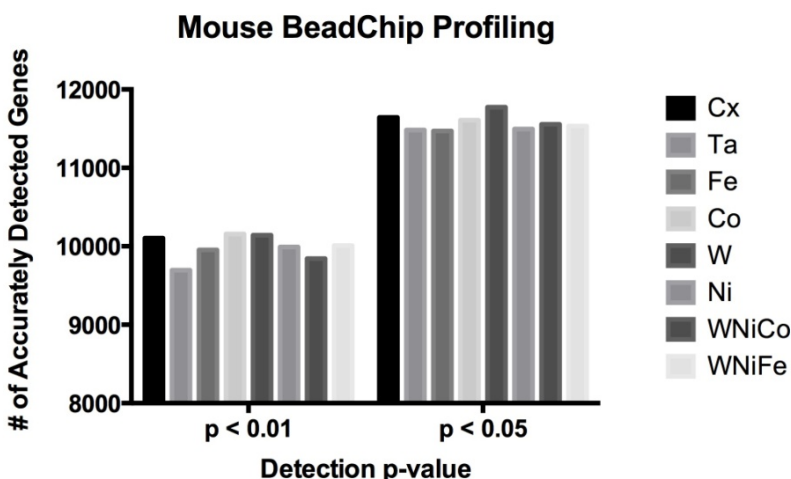
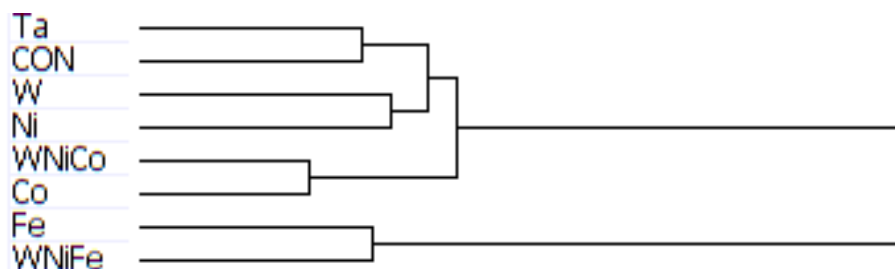


Table 3. Mouse data comparison between actual numbers of features accurately expressed in each exposure group at the detection p -value ≤ 0.05 and ≤ 0.01 .

	Cx	Ta	Fe	Co	W	Ni	WNiCo	WNiFe
$p \leq 0.05$	11,643	11,483	11,469	11,608	11,772	11,496	11,555	11,533
$p \leq 0.01$	10,103	9695	9953	10,157	10,142	9990	9843	10,008

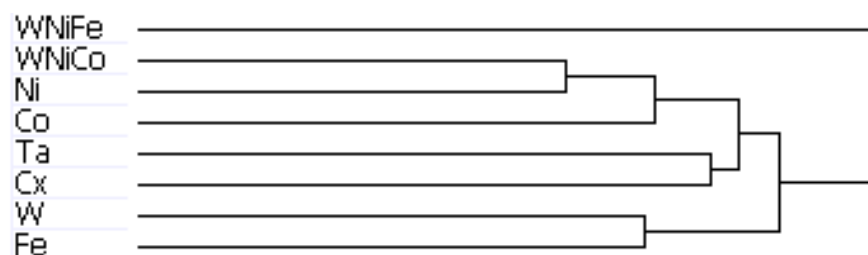
3.3. Hierarchical Clustering Analysis of Exposure Groups

Complete transcriptome signatures can be clustered to determine similarity in cellular response to external stimuli, such as small molecular exposure. We hypothesized that metal exposure with similar tumorigenic outcomes would be associated with similar transcriptome signatures as profiled by BeadArray. Thus, we used unbiased hierarchical clustering of gene expression levels from accurately detected features of the BeadChip to classify exposure samples by groups. Hierarchical clustering analysis of the mouse data produced a dendrogram showing groupings of like metals, with Ta and the control group on the same branch, W and Ni one branch, Co and WNiCo on one branch, and Fe and WNiFe on a separate branch (Figure 3). While the variable groupings appear consistent with known effects, the short length of the branches suggests the differences between the groups are small and that there was not a large effect of metal exposure after 24 h. Ratio comparisons done between Ta and WNiCo groups from the mouse microarray data did not show fold changes greater than 1.35 among features accurately detected in all eight groups, further supporting the suggestion that there was not a significant difference between the exposure groups after 24 h.

Figure 3. Dendrogram from hierarchal clustering analysis of mouse microarray data.

The results of hierarchal clustering on the rat dataset showed that after 24 h of exposure, metal groups with similar tumor-producing properties, such as WNiCo and Ni, and Ta and the untreated control group (Cx) aligned on near-branches of the dendrogram. Interestingly, exposure groups believed to have dissimilar genotoxic properties, such as W and Fe aligned on near branches (Figure 4). According to the dendrogram, these groupings suggest that W alone and Fe alone are more different than WNiCo and Ni alone. It also suggests that effects observed in the WNiCo group may be attributed more to Ni than W after 24 h exposure.

The rat dendrogram (Figure 4) revealed two distinct group pairings on different arms, Ta and Cx on one arm, and Ni and WNiCo on another arm. Additionally, the longer branch arms indicate a greater effect of the metals on the rat cells than was observed in the mouse samples. The WNiFe exposure group was a distinct outlier from all other groups in that the gene expression of this group was distinctively dissimilar from all other groups.

Figure 4. Dendrogram from hierarchal clustering analysis of rat microarray data.

The arrangement of the dendrogram clustering was consistent for both the rat and mouse datasets, regardless of the cutoff parameters used to run the hierarchical clustering analysis: the complete genome, a data set of genes accurately expressed in at least one group, accurately expressed in 6, 7 or 8 groups, or the dataset consisting of genes accurately expressed in all eight groups. This indicates that the changes in gene expression observed between the different exposure groups is consistent within the dataset, regardless of the number of accurately detected probes used in the analysis.

3.4. Comparative Marker Selection and Ratio Analysis

Unbiased hierarchical clustering led us to hypothesize that the most significant differences would be observed when comparing non-tumor (Ta and Cx) to tumor (W, Ni) groups. However, while the dendrogram of the mouse dataset showed promise, comparative marker selection analysis failed to show any significantly differentially-expressed genes ($p < 0.05$; fold change greater than 1.35) between the two classes. Additionally, ratios run between the average signals of Tumor (W, Ni) and Non-tumor (Ta and Cx) groups failed to show any fold change greater than 1.35 between the two groups. The lack of significant differences between the average signals of accurately detected probes indicates a low level of altered gene expression between the groups following 24 h exposure to the metals.

Led by the same hypothesis as for the mouse-specific analysis and based on results from *in vivo* studies that demonstrated that WNiCo and Ni exposure produced tumors while other metal exposures did not [22,25], two classes of groups were created within the rat dataset: Tumor (W, Ni, WNiCo), and Non-tumor (Ta, Fe, Cx). WNiFe and Co, the two sample groups least like the others in the hierarchical cluster analysis, were excluded. A comparative marker selection analysis was run to determine the number of differentially expressed genes between the two classes.

Comparative marker selection analysis results were filtered for fold changes of genes between exposure groups of ≥ 1.35 with a p -value ≤ 0.05 . Results showed upregulation of 10 genes in the “Non-tumor” class, or NON (Cx, Ta, Fe), and 14 genes in the “Tumor” class, or TUM (W, Ni, WNiCo). The fold change, probe ID number, and gene name are shown in Table 4.

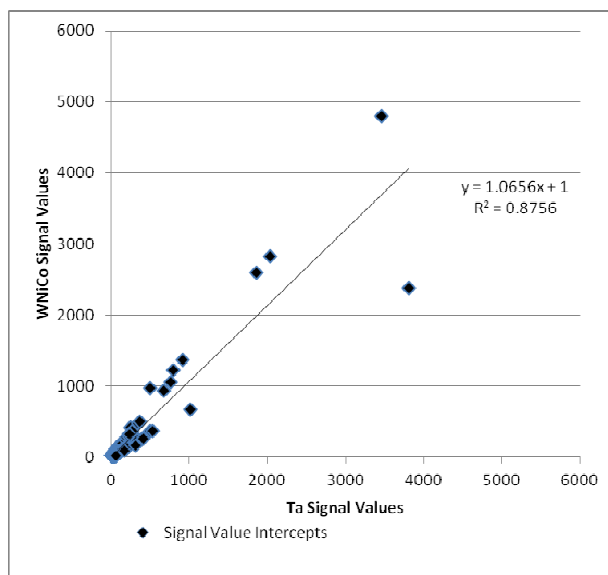
Additionally, the Ta and WNiCo groups were selected to represent each class in pairwise analysis. Genes that were accurately detected in both Ta and WNiCo that had a ratio indicating fold change between the two groups of ≥ 1.35 or its inverse ≤ 0.74 were selected to determine amount of fold change between the two groups and plotted (Figure 5). Nine hundred and sixteen (916) genes met these criteria; 469 that showed a higher level of gene expression in the WNiCo group, and 447 that showed a higher level of gene expression in the Ta group. If the data points make a straight line going from the origin out to high x- and y-values, then the variables are said to have a positive correlation. In this case, the

data points that are outliers from the trendline are of interest, because these points indicate that the gene expression values are substantially different, which is what would be expected if there is a significant difference in effect size between WNiCo and Ta exposures.

Table 4. Results of CMS analysis between Non-tumor class (NON) and Tumor class (TUM), showing those genes which showed a > 1.50 fold change between the two groups.

Upregulated in Class	Probe ID	Gene Name	Fold Change
NON	ILMN_1366318	RGD1306926_PREDICTED	1.68
NON	ILMN_1376639	DYX1C1	1.42
NON	ILMN_1359445	KCNJ9	1.86
NON	ILMN_1352946	ZBED3	1.51
NON	ILMN_1373980	CDGAP_PREDICTED	1.36
NON	ILMN_1649958	LOC294726	1.36
NON	ILMN_1376505	TLL1	1.64
NON	ILMN_1361716	LGALS2	1.36
NON	ILMN_1375469	RGD1307826_PREDICTED	1.38
NON	ILMN_1354019	SARDH	1.44
TUM	ILMN_1367175	RGD1562265_PREDICTED	1.37
TUM	ILMN_1363142	NMT2	1.49
TUM	ILMN_1350240	RGD1311358	1.37
TUM	ILMN_1353413	RGD1308106_PREDICTED	1.58
TUM	ILMN_1358380	CNOT3_PREDICTED	1.37
TUM	ILMN_1360156	RGD1562716_PREDICTED	1.47
TUM	ILMN_1364447	MLANA_PREDICTED	1.51
TUM	ILMN_1368669	RGD1564211_PREDICTED	1.43
TUM	ILMN_1368356	FOS	1.70
TUM	ILMN_1369005	EGR1	1.47
TUM	ILMN_1351892	RGD1560234_PREDICTED	1.49
TUM	ILMN_1362498	ZFP84_PREDICTED	1.40
TUM	ILMN_1362589	CWF19L1_PREDICTED	1.36
TUM	ILMN_1376212	ACE2	1.52

Figure 5. Plot of WNiCo and Ta signal values for fold change ≥ 1.35 and ≤ 0.74 .



3.5. PCR Analysis

To validate the microarray results of the rat cell samples, we utilized quantitative real-time PCR analysis, a gold-standard independent methodology with ability to detect minimal fold-changes in expression. Six genes were selected from the microarray data that showed a fold change greater than 1.35 between Ta and WNiCo; three with greater expression in the Ta group (AP2A1, CHRND, FBXW5), and three with greater expression in the WNiCo group (FN3K, GALNT2 POLR3E) (Table 5). Additionally, three genes (FOS, EGR1 and NMT2) were selected that were among the CMS results. All but two of the genes (CHRND and FN3K) were accurately detected in all eight exposure groups, with CHRND accurately detected in six groups (all except for W and WNiCo groups), and FN3K, which was accurately detected in three groups (Ta, Fe and WNiCo groups) (Table 5). Paired *t*-test *p*-values for the effect of WNiCo and Ta were found to be consistent with the microarray data. Four genes (AP2A1, CHRND, FN3K and GALNT2) were differently expressed at statistically significant levels between the exposure groups using 2-tailed *t*-tests ($p = 0.03$), and directionality of expression differences were validated in six of the genes (AP2A1, CHRND, FBXW5, FN3K, POLR3E). However, for two genes (GALNT2 and POLR3E), PCR expression directionality was reverse of the microarray results (Figure 6). A two-tailed *t*-test between CHRND expression in WNiCo and Ta, and between WNiCo and Cx showed significance ($p < 0.03$ and $p < 0.05$, respectively), indicating a difference in expression between the WNiCo group and both Ta and Cx. AP2A1, FN3K and GALNT2 showed similar results for WNiCo and Ta ($p < 0.03$, $p < 0.04$, and $p < 0.04$ respectively). Based on this information, it was concluded that the expression values and fold changes observed in microarray data correlated with PCR results.

Table 5. Genes selected for PCR validation, with rat microarray average signal values.

ACCESSION	SYMBOL	Cx	Ta	Co	W	Ni	WNiCo	WNiFe
XM_001078388.1	AP2A1	45.70	57.40	41.10	48.00	43.70	25.30	36.40
NM_019298.1	CHRND	26.90	22.80	19.50	23.80	10.50	7.40	17.50
NM_001025730.1	FBXW5	96.10	74.30	60.90	66.50	75.40	43.00	57.40
XM_573235.2	FN3K	5.80	15.20	-2.80	11.70	9.30	26.20	10.10
XM_001054081.1	GALNT2	38.80	20.20	35.10	31.10	27.70	50.10	31.10
XM_001075970.1	POLR3E	35.60	47.00	67.10	39.90	47.40	75.50	63.60
NM_022197.1	FOS	27.50	19.10	18.60	34.20	44.90	47.60	40.00
NM_012551.1	EGR1	209.60	253.10	296.50	367.60	429.80	415.90	426.60
NM_207590.1	NMT2	15.30	20.60	20.30	37.20	22.90	28.70	29.80

3.6. Genes of Interest

Of the genes that were selected from the rat dataset for validation via qPCR, several are known to be associated with tumorigenic pathways, apoptosis, or cellular repair. Of particular interest were the genes CHRND, EGR1, FN3K, FOS and NMT2 (Table 6).

Figure 6. PCR expression values for selected genes for the Ta control and WNiCo groups. Data are the mean of three measurements. Error bars represent standard error.

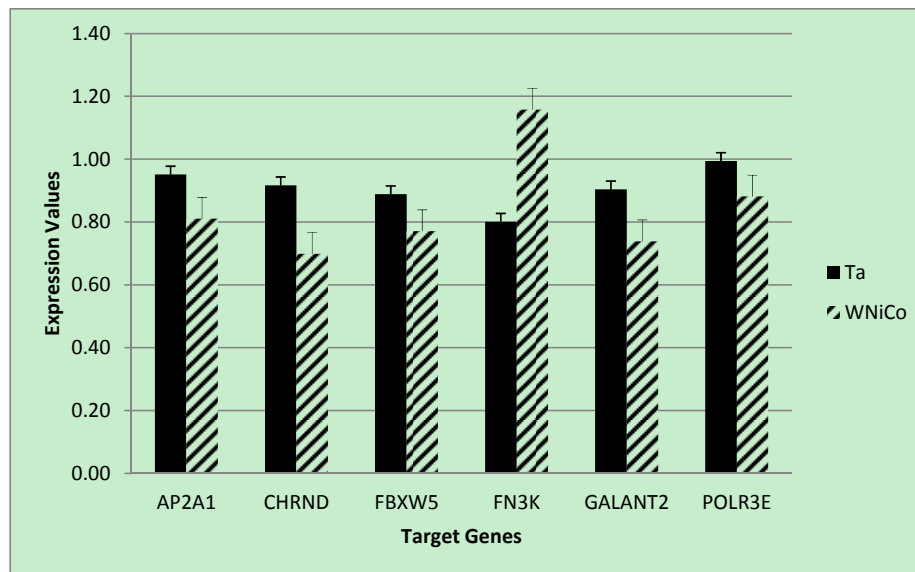


Table 6. Validated genes found to be associated with genotoxic pathways.

Gene	Name	Accession #
CHRND	Chrnd cholinergic receptor, nicotinic, delta	NM_019298.1
EGR1	Egr1 early growth response 1	NM_012551.1
FN3K	Fructosamine 3 kinase	NM_001109051.1
FOS	Fos FBJ murine osteosarcoma viral oncogene homolog	NM_022197.2
NMT2	N-myristoyltransferase 2	NM_207590.1

Nicotinic cholinergic receptor subunit delta (CHRND), was accurately detected in six of eight groups, and was differentially expressed to a greater extent in the Ta group as opposed to the WNiCo group, with a fold change of 3.08. EGR1 was accurately detected in all eight exposure groups, with an upregulated fold change of 1.6 more in the WNiCo group than in Ta group. While the PCR validated the expression, if not the directionality in both the Ta and WNiCo groups, *t*-test results showed no statistically significant difference between the expression values of two groups in the PCR results. Numerically, the average expression value of the Ta and Cx groups were very close (0.97 and 0.95, respectively); expression was slightly higher in WNiCo (1.02) than both Ta and Cx values.

Analysis of the microarray data showed FOS upregulated in the tumor class of the CMS with a fold change of 1.7, and a fold change 2.5 times higher in WNiCo than Ta. There was no statistical difference in expression between WNiCo and Ta in the PCR results, although both were validated by the test, and the average of the WNiCo results were higher than both Ta and Cx.

FN3K was upregulated in the tumor class in the CMS data, and in WNiCo alone with a fold change of 1.7 times greater in WNiCo than in Ta. A *t*-test between the Ta and the WNiCo group PCR results showed statistically significant differences in the expression of FN3K in the WNiCo groups over the Ta groups ($p = 0.03$).

4. Discussion

The purpose of this study was to look at very early events occurring at the genetic level in cultured rodent muscle cells after exposure to tungsten alloys and their individual component metals, with the aim of identifying early changes that might contribute to the development of metal-induced tumors. It was found that after 24 h of exposure to the different metal groups, subtle changes in gene expression between the exposure groups were observed in the rat muscle cells, but were not seen in the mouse muscle cells. Differences in the species' genetic response to metal exposure may account for this, and longer exposure intervals would be required to see if changes in expression become more pronounced over time.

Hierarchical clustering analysis yielded consistent results showing similarities between the basic networks of samples. For the mouse dataset, while Ta and Cx, and W and Ni, paired together on unique branches, WNiCo and Co consistently paired on a separate branch, and Fe and WNiFe paired on a branch independent from the others. For the rat dataset, Ta and Cx, Ni and WNiCo, and W and Fe consistently showed up paired together on different arms of the dendrogram hierarchy, indicating Ta and Cx displayed similarities, and were sufficiently dissimilar to Ni and WNiCo, which showed similarities to each other. Co showed some similarity to Ni and WNiCo, and they were on the same branch. WNiFe was an outlier, showing up on a completely separate arm from all other groups.

As was indicated in the results section, this information initially looked promising, but further analysis of the mouse data showed only very small expression differences between the groups as evidenced by fold changes of less than 1.35 and the small number of accurately detected probes, indicating that after 24 h exposure, there was not very much activity stimulated by exposure to the metals. This may be due to a delayed response in mouse cells to exposure to the metals, a higher tolerance than rat cells to metal toxicity, or a better adaptation mechanism than rat cells. Current research [33] has shown that mice implanted with WNiCo pellets eventually develop rhabdomyosarcomas, but the time to tumor formation is far longer (12–15 months) than that seen for WNiCo-implanted rats (3 months) [25]. This suggests that mice may have a protective mechanism that impedes the genetic damage leading to tumorigenesis until later in their lifecycle, at which time it either shuts off, or is overwhelmed by the metal exposure. Whatever the cause, further study utilizing both *in vitro* and *in vivo* model systems is warranted.

Since the differential changes between control and metal-treated mouse cells were not statistically significant, genes for PCR validation were selected from the rat microarray data set where probe IDs were accurately expressed in all eight groups. The genes were selected for signal strength rather than gene function in order to validate overall gene expression in the microarray data using real time qPCR, considered the gold standard for gene expression validation. This process was part of the discovery process, and helped to validate the overall microarray data. None of the genes showed a fold change greater than 2.50, but while the differences in expression between the different groups was subtle, it is important to note that changes were observed, indicating that there are metal-induced changes occurring in the rat muscle cells as soon as 24 h after exposure.

Three genes were validated in the qPCR showing both directionality and statistically significant differences—AP2A1, CHRND and FN3K. AP2A1 (adaptor-related protein complex) is associated with endocytosis, protein transport, cargo selection and vesicle formation, but does not appear to be

directly associated with tumorigenic pathways [34]. FN3K (fructosamine 3 kinase) is involved in cellular repair, maintenance and defense against toxins, primarily repairing protein damage caused by glucose, and is responsible for protein deglycation, and considered a housekeeping gene in cellular maintenance [35].

Interestingly, CHRND, a member of the nicotinic acetylcholine receptor family, is a recognized candidate for tumor associated rearrangements and as one of the muscle-specific genes that is expressed in rhabdomyosarcomas [36,37]. It is considered diagnostic tumor marker [36,38]. However, while the difference in CHRND expression between Ta and WNiCo was statistically significant, the expression value was higher in the Ta group than the WNiCo group. One possible explanation for this is that the gene may initially be suppressed early in the response to WNiCo exposure. To evaluate adequately, it would be necessary to follow CHRND expression across longer exposure times or to utilize tumor tissue from animal studies.

Identification of genes within known tumorigenic or tumor suppression pathways that either up-regulate or down-regulate in response to metal exposure is crucial in understanding the impact of long-term exposure to embedded metals, including the tungsten alloys. Correlation of early genetic changes in an *in vitro* model with known tumorigenic outcomes in an *in vivo* model will provide the information needed to make informed decisions on the proper treatment of embedded metal fragment wounds. Of the genes identified in the rat microarray data and validated via qPCR, several bear further investigation as they may indicate initiation of oncogenic processes that correlate with metal exposure. They include EGR1, FOS, FN3K, and NMT2.

EGR1 is essential for mediation of the p53-independent c-Myc-induced apoptosis. It is also implicated in progression of certain types of prostate cancers, and possibly implicated in tumor suppression [39]. The expression of EGR1 and the slight difference between the tumor and non-tumor groups may allude to the possibility of a greater difference in expression between the groups. Even this slight difference in expression of the gene between these groups after only 24 h may indicate that cellular damage and the initiation of oncogenic pathways is occurring almost immediately after exposure.

FOS (FBJ osteosarcoma oncogene) is a canonical oncogene, and is part of the AP-1 transcription factor, which upregulates transcription of genes involved in proliferation, differentiation and defense against invasion and cell damage. It is associated with cell transformation and progression of cancer. Interestingly, a recent study showed that the disruption of certain oncosuppression transcripts have been shown to induce both FOS and EGR1 expression in the early stages of tumor development [40]. FN3K (FNSK) is considered a housekeeping gene that is activated in response to an increase in interleukin 1 β . It involved in cellular repair in response to glucose-related protein damage. Specifically, it catalyzes phosphorylation of fructosamines that are formed by glycation, the nonenzymatic reaction of glucose [35,41]. Expression of this gene in the WNiCo exposure group may indicate early cellular damage that initiates a cellular repair process soon after exposure.

NMT2 is also associated with oncogenic pathways. It is part of the gene group associated with myristoylation (irreversible protein modification) [42]. There is some evidence that NMT2 may play a role in the pathogenesis of human colorectal cancer. Interestingly, the expression of NMT2 is rapidly upregulated within minutes in response to inflammatory signals, a component of tumorigenesis [43].

Furthermore, NMT2 induction (activation by a molecule inactivating a repressor gene) in direct response to carcinogen exposure (dioxins) has also been demonstrated [44].

5. Conclusions

While the recent interest over the effects of tungsten alloys has largely focused on their effects on muscle tissue, it is becoming increasingly evident that these alloys have toxic effects on other physiologic systems, and gene expression profiles are consistent with some of the results observed in this study. Recent research on the effects of inhaled WNiCo showed a dose-dependent inflammatory response that resulted in the expression of genes associated with apoptosis, DNA damage and repair, and carcinogenesis [45]. WNiCo was also recently shown to have cytotoxic effects on human brain and kidney cells at a greater rate than W alone [46]. Clearly, additional research is needed to assess the cytotoxic and genotoxic effects of tungsten alloy exposure occurring by various routes of internalization.

Acknowledgments

The views expressed do not necessarily represent the Armed Forces Radiobiology Research Institute, the Daniel K. Inouye Graduate School of Nursing, the Uniformed Services University of the Health Sciences, the United States Public Health Service, or the United States Departments of Defense and Veterans Affairs. This material is based upon work supported in part by the Department of Veterans Affairs, Veterans Health Administration, Office of Research and Development Rehabilitation Research and Development Service B5044R to Kasper and USUHS Graduate Student Award T061M8 to Bardack.

Author Contributions

All work reported in this paper was performed at USUHS. John F. Kalinich, Clifton L. Dalgard, and Christine E. Kasper supervised the study and had access to all data throughout the study period and take responsibility for the integrity and accuracy of the data analysis. Stephanie Bardack conducted the experiments with the assistance of John F. Kalinich and Christine E. Kasper; and, analyzed the data with the assistance of Clifton L. Dalgard.

Conflicts of Interest

The authors declare no conflict of interest.

References

1. Daxon, E.G.; Musk, J.H. Assessment of the Risks from Imbedded Fragments of Depleted Uranium. In *AFRRRI Technical Report TR93-1*; Armed Forces Radiobiology Research Inst.: Bethesda, MD, USA, 1993; p. 28.
2. Hahn, F.F.; Guilmette, R.A.; Hoover, M.D. Implanted depleted uranium fragments cause soft tissue sarcomas in the muscles of rats. *Environ. Health Perspect.* **2002**, *110*, 51–59.

3. Hodge, S.J.; Ejniak, J.; Squibb, K.S.; McDiarmid, M.A.; Morris, E.R.; Landauer, M.R.; McClain, D.E. Detection of depleted uranium in biological samples from Gulf War veterans. *Mil. Med.* **2001**, *166*, 69–70.
4. Miller, A.C.; Blakely, W.F.; Livengood, D.; Whittaker, T.; Xu, J.; Ejniak, J.W.; Hamilton, M.M.; Parlette, E.; John, T.S.; Gerstenberg, H.M.; Hsu, H. Transformation of human osteoblast cells to the tumorigenic phenotype by depleted uranium-uranyl chloride. *Environ. Health Perspect.* **1998**, *106*, 465–471.
5. Miller, A.C.; Fuciarelli, A.F.; Jackson, W.E.; Ejniak, E.J.; Emond, C.; Strocko, S.; Hogan, J.; Page, N.; Pellmar, T. Urinary and serum mutagenicity studies with rats implanted with depleted uranium or tantalum pellets. *Mutagenesis* **1998**, *13*, 643–648.
6. McClain, D.E.; Benson, K.A.; Dalton, T.K.; Ejniak, J.; Emond, C.A.; Hodge, S.J.; Kalinich, J.F.; Landauer, M.A.; Miller, A.C.; Pellmar, T.C.; *et al.* Biological effects of embedded depleted uranium (DU): Summary of Armed Forces Radiobiology Research Institute research. *Sci. Total Environ.* **2001**, *274*, 115–118.
7. McClain, D.E.; Benson, K.A.; Dalton, T.K.; Ejniak, J.; Emond, C.A.; Hodge, S.J.; Kalinich, J.F.; Landauer, M.R.; Livengood, D.R.; Miller, A.C.; *et al.* Health effects of embedded depleted uranium. *Mil. Med.* **2002**, *167*, 117–119.
8. McClain, D.E.; Miller, A.C.; Kalinich, J.F. Status of Health Concerns about Military Use of Depleted Uranium and Surrogate Metals in Armor-Penetrating Munitions. In Proceedings of the Human Factors and Medicine Panel Research Task Group 099 “Radiation Bioeffects and Countermeasures” Meeting, Bethesda, MD, USA, 21–23 June 2005; Armed Forces Radiobiology Research Institute: Bethesda, MD, USA, 2005.
9. McDiarmid, M.A.; Keogh, J.P.; Hooper, F.J.; McPhaul, K.; Squibb, K.; Kane, R.; DiPino, R.; Kabat, M.; Kaup, B.; Anderson, L.; *et al.* Health effects of depleted uranium on exposed Gulf War veterans. *Environ. Res.* **2000**, *82*, 168–180.
10. McDiarmid, M.A. Depleted uranium and public health. *Br. Med. J.* **2001**, *322*, 123–124.
11. McDiarmid, M.A.; Squibb, K.; Engelhardt, S.; Oliver, M.; Gucer, P.; Wilson, P.D.; Kane, R.; Kabat, M.; Kaup, B.; Anderson, L.; *et al.* Surveillance of depleted uranium exposed Gulf War veterans: Health effects observed in an enlarged “friendly fire” cohort. *J. Occup. Environ. Med.* **2001**, *43*, 991–1000.
12. McDiarmid, M.A.; Hooper, F.J.; Squibb, K.; McPhaul, K.; Engelhardt, S.M.; Kane, R.; DiPino, R.; Kabat, M. Health effects and biological monitoring results of Gulf War veterans exposed to depleted uranium. *Mil. Med.* **2002**, *167*, 123–124.
13. McDiarmid, M.A.; Engelhardt, S.; Oliver, M.; Gucer, P.; Wilson, P.D.; Kane, R.; Kabat, M.; Kaup, B.; Anderson, L.; Hoover, D.; *et al.* Health effects of depleted uranium on exposed Gulf War veterans: A 10-year follow-up. *J. Toxicol. Environ. Health A* **2004**, *67*, 277–296.
14. Miller, A.C.; Xu, J.; Stewart, M.; Prasanna, P.G.S.; Page, N. Potential late health effects of depleted uranium and tungsten used in armor-piercing munitions: Comparison of neoplastic transformation and genotoxicity with the known carcinogen nickel. *Mil. Med.* **2002**, *167*, 120–122.

15. Miller, A.C.; Brooks, K.; Stewart, M.; Anderson, B.; Shi, L.; McClain, D.; Page, N. Genomic instability in human osteoblast cells after exposure to depleted uranium: Delayed lethality and micronuclei formation. *J. Environ. Radioact.* **2003**, *64*, 247–259.
16. Miller, A.C.; Brooks, K.; Smith, J.; Page, N.; Miller, A.C.; Brooks, K.; Smith, J.; Page, N. Effect of the militarily-relevant heavy metals, depleted uranium and heavy metal tungsten-alloy on gene expression in human liver carcinoma cells (HepG2). *Mol. Cell. Biochem.* **2004**, *255*, 247–256.
17. Miller, A.C.; Beltran, D.; Rivas, R.; Stewart, M.; Merlot, R.J.; Lison, P.B. Radiation- and Depleted Uranium-Induced Carcinogenesis Studies: Characterization of the Carcinogenic Process and Development of Medical Countermeasures. In Proceedings of the Human Factors and Medicine Panel Research Task Group 099 “Radiation Bioeffects and Countermeasures” Meeting, Bethesda, MD, USA, 21–23 June 2005; Armed Forces Radiobiology Research Institute: Bethesda, MD, USA, 2005.
18. Miller, A.C.; Bonait-Pellie, C.; Merlot, R.F.; Michel, J.; Stewart, M.; Lison, P.D. Leukemic transformation of hematopoietic cells in mice internally exposed to depleted uranium. *Mol. Cell. Biochem.* **2005**, *279*, 97–104.
19. Pellmar, T.C.; Fuciarelli, A.F.; Ejniak, J.W.; Hamilton, M.; Hogan, J.; Strocko, S.; Emond, C.; Mottaz, H.M.; Landauer, M.R. Distribution of uranium in rats implanted with depleted uranium pellets. *Toxicol. Sci.* **1999**, *49*, 29–39.
20. Squibb, K.S.; McDiarmid, M.A. Depleted uranium exposure and health effects in Gulf War veterans. *Philos. Trans. R. Soc. Lond. B Biol. Sci.* **2006**, *361*, 639–648.
21. Davitt, R.P. A Comparison of the Advantages and Disadvantages of Depleted Uranium and Tungsten Alloy as Penetrator Materials. In *Tank Ammo Section Report No. 107*; US Army Armament Research and Development Command: Dover, NJ, USA, 1980; p. 32.
22. Miller, A.C.; Mog, S.; McKinney, L.; Luo, L.; Allen, J.; Xu, J.; Page, N. Neoplastic transformation of human osteoblast cells to the tumorigenic phenotype by heavy metal-tungsten alloy particles: Induction of genotoxic effects. *Carcinogenesis* **2001**, *22*, 115–125.
23. van der Voet, G.B.; Todorov, T.I.; Centeno, J.A.; Jonas, W.; Ives, J.; Mullick, F.G. Metals and health: A clinical toxicological perspective on tungsten and review of the literature. *Mil. Med.* **2007**, *172*, 1002–1005.
24. Kalinich, J.F.; Emond, C.A.; Dalton, T.K.; Mog, S.R.; Coleman, G.D.; Kordell, J.E.; Miller, A.C.; McClain, D.E. Embedded weapons-grade tungsten alloy shrapnel rapidly induces metastatic high-grade rhabdomyosarcomas in F344 rats. *Environ. Health Perspect.* **2005**, *113*, 729–734.
25. Gold, K.; Cheng, Y.S.; Holmes, T.D. A quantitative analysis of aerosols inside an armored vehicle perforated by a kinetic energy penetrator containing tungsten, nickel, and cobalt. *Mil. Med.* **2007**, *172*, 393–398.
26. DoD(HA). *DoD(HA) Policy on Analysis of Metal Fragments Removed from Department of Defense Personnel*; Policy Letter 07–029; Office of the Assistant Secretary for Health Affairs: Washington, DC, USA, 2007.
27. Kane, M.A.; Kasper, C.E.; Kalinich, J.F. The use of established skeletal muscle cell lines to assess potential toxicity from embedded metal fragments. *Toxicol. In Vitro* **2009**, *23*, 356–359.

28. Reich, M.; Liefeld, T.; Gould, J.; Lerner, J.; Tamayo, P.; Mesirov, J.P. GenePattern 2.0. *Nat. Genet.* **2006**, *38*, 500–501.
29. Schuster, B.E.; Roszell, L.E.; Murr, L.E.; Ramirez, D.A.; Demaree, J.D.; Klotz, B.R.; Rosencrance, A.B.; Dennis, W.E.; Bao, W.; Perkins, E.J.; *et al.* *In vivo* corrosion, tumor outcome, and microarray gene expression for two types of muscle-implanted tungsten alloys. *Toxicol. Appl. Pharmacol.* **2012**, *265*, 128–138.
30. Hockley, A.D.; Goldin, J.H.; Wake, M.J.; Iqbal, J. Skull repair in children. *Pediatr. Neurosurg.* **1990**, *16*, 271–275.
31. Johansson, C.B.; Hansson, H.A.; Albrektsson, T. Qualitative interfacial study between bone and tantalum, niobium or commercially pure titanium. *Biomaterials* **1990**, *11*, 277–280.
32. Fan, J.B.; Gunderson, K.L.; Bibikova, M.; Yeakley, J.M.; Chen, J.; Wickham Garcia, E.; Lebruska, L.L.; Laurent, M.; Shen, R.; Barker, D. Illumina universal bead arrays. *Methods Enzymol.* **2006**, *410*, 57–73.
33. Emond, C.E.; Vergara, V.B.; Lombardini, E.D.; Kalinich, J.F. Induction of Rhabdomyosarcoma by embedded Tungsten/Nickel/Cobalt but not by Tungsten/Nickel/Iron in the B6C3F1 mouse. 2014, In preparation.
34. Rotem-Yehudar, R.; Galperin, E.; Horowitz, M. Association of insulin-like growth factor 1 receptor with EHD1 and SNAP29. *J. Biol. Chem.* **2001**, *276*, 33054–33060.
35. Conner, J.R.; Beisswenger, P.J.; Szwergold, B.S. Some clues as to the regulation, expression, function, and distribution of fructosamine-3-kinase and fructosamine-3-kinase-related protein. *Ann. N. Y. Acad. Sci.* **2005**, *1043*, 824–836.
36. Grassi, F.; Bouche, M.; Aguanno, S.; Molinaro, M.; Eusebi, F. Single acetylcholine-activated channels in cultured rhabdomyoblasts. *Exp. Cell Res.* **1987**, *171*, 498–502.
37. Barr, F.G.; Biegel, J.A.; Sellinger, B.; Womer, R.B.; Emanuel, B.S. Molecular and cytogenetic analysis of chromosomal arms 2q and 13q in alveolar rhabdomyosarcoma. *Genes Chromosomes Cancer* **1991**, *3*, 153–161.
38. Luther, M.A.; Schoepfer, R.; Whiting, P.; Casey, B.; Blatt, Y.; Montal, M.S.; Montal, M.; Linstrom, J. A muscle acetylcholine receptor is expressed in the human cerebellar medulloblastoma cell line TE671. *J. Neurosci.* **1989**, *9*, 1082–1096.
39. Boone, D.N.; Qi, Y.; Li, Z.; Hann, S.R. Egr1 mediates p53-independent c-Myc-induced apoptosis via a noncanonical ARF-dependent transcriptional mechanism. *Proc. Natl. Acad. Sci. USA* **2011**, *108*, 632–637.
40. Schiavone, D.; Avalle, L.; Dewilde, S.; Poli, V. The immediate early genes Fos and Egr1 become STAT1 transcriptional targets in the absence of STAT3. *FEBS Lett.* **2011**, *585*, 2455–2460.
41. Delplanque, J.; Delpierre, G.; Opperdoes, F.R.; Van Schaftingen, E. Tissue distribution and evolution of fructosamine 3-kinase and fructosamine 3-kinase-related protein. *J. Biol. Chem.* **2004**, *279*, 46606–46613.
42. Rioux, V.; Beauchamp, E.; Pedrono, F.; Daval, S.; Molle, D.; Catheline, D.; Legrand, P. Identification and characterization of recombinant and native rat myristoyl-CoA: Protein N-myristoyltransferases. *Mol. Cell. Biochem.* **2006**, *286*, 161–170.

43. Shrivastav, A.; Suri, S.S.; Mohr, R.; Janardhan, K.S.; Sharma, R.K.; Singh, B. Expression and activity of N-myristoyltransferase in lung inflammation of cattle and its role in neutrophil apoptosis. *Vet. Res.* **2010**, *41*, 9.
44. Kolluri, S.K.; Balduf, C.; Hofmann, M.; Gottlicher, M. Novel target genes of the Ah (dioxin) receptor: Transcriptional induction of N-myristoyltransferase 2. *Cancer Res.* **2001**, *61*, 8534–8539.
45. Roedel, E.Q.; Cafasso, D.E.; Lee, K.W.; Pierce, L.M. Pulmonary toxicity after exposure to military-relevant heavy metal tungsten alloy particles. *Toxicol. Appl. Pharmacol.* **2011**, *259*, 74–86.
46. Verma, R.; Xu, X.; Jaiswal, M.K.; Olsen, C.; Mears, D.; Caretti, G.; Galdzicki, Z. *In vitro* profiling of epigenetic modifications underlying heavy metal toxicity of tungsten-alloy and its components. *Toxicol. Appl. Pharmacol.* **2011**, *253*, 178–187.

© 2014 by the authors; licensee MDPI, Basel, Switzerland. This article is an open access article distributed under the terms and conditions of the Creative Commons Attribution license (<http://creativecommons.org/licenses/by/3.0/>).